MYELOID NEOPLASIA

Reprogramming identifies functionally distinct stages of clonal evolution in myelodysplastic syndromes

Jasper Hsu,[1] Andreea Reilly,[1] Brian J. Hayes,[2] Courtnee A. Clough,[1] Eric Q. Konnick,[3] Beverly Torok-Storb,[2] Suleyman Gulsuner,[4] David Wu,[3] Pamela S. Becker,[1,2,5] Siobán B. Keel,[1] Janis L. Abkowitz,[1,5,6] and Sergei Doulatov[1,5,6]

[1]Division of Hematology, Department of Medicine, University of Washington, Seattle, WA; [2]Fred Hutchinson Cancer Research Center, Seattle, WA; and [3]Department of Laboratory Medicine, [4]Division of Medical Genetics, Department of Medicine, [5]Institute for Stem Cell and Regenerative Medicine, and [6]Department of Genome Sciences, University of Washington, Seattle, WA

KEY POINTS

- **Reprogramming identifies clonal history and recapitulates disease progression in individual patients with MDS.**

- **Mitochondrial function and chromosome stability are key pathways affected by acquisition of mutations in MDS.**

Myeloid neoplasms, including myelodysplastic syndromes (MDS), are genetically heterogeneous disorders driven by clonal acquisition of somatic mutations in hematopoietic stem and progenitor cells (HPCs). The order of premalignant mutations and their impact on HPC self-renewal and differentiation remain poorly understood. We show that episomal reprogramming of MDS patient samples generates induced pluripotent stem cells from single premalignant cells with a partial complement of mutations, directly informing the temporal order of mutations in the individual patient. Reprogramming preferentially captured early subclones with fewer mutations, which were rare among single patient cells. To evaluate the functional impact of clonal evolution in individual patients, we differentiated isogenic MDS induced pluripotent stem cells harboring up to 4 successive clonal abnormalities recapitulating a progressive decrease in hematopoietic differentiation potential. SF3B1, in concert with epigenetic mutations, perturbed mitochondrial function leading to accumulation of damaged mitochondria during disease progression, resulting in apoptosis and ineffective erythropoiesis. Reprogramming also informed the order of premalignant mutations in patients with complex karyotype and identified 5q deletion as an early cytogenetic anomaly. The loss of chromosome 5q cooperated with _TP53_ mutations to perturb genome stability, promoting acquisition of structural and karyotypic abnormalities. Reprogramming thus enables molecular and functional interrogation of preleukemic clonal evolution, identifying mitochondrial function and chromosome stability as key pathways affected by acquisition of somatic mutations in MDS. (_Blood_. 2019;134(2):186-198)

Introduction

Cancer can be viewed as a Darwinian evolutionary process driven by acquisition of somatic mutations and subclonal selection.[1] Hematologic malignancy is often preceded by a period of clonal evolution, or clonal hematopoiesis (CH), during which hematopoietic stem and progenitors accumulate oncogenic mutations.[2,3] These early preleukemic events confer increased self-renewal and acquire cooperating mutations. Myelodysplastic syndrome (MDS), often the first clinical diagnosis, is characterized by clonal stem cell expansion and impaired differentiation into one or more myeloid cell lineage. The identity and prognostic significance of recurrent oncogenic changes in MDS are relatively well established.[4] These include point mutations in epigenetic regulators (eg, _TET2_, _DNMT3A_), the spliceosome (eg, _SF3B1_, _SRSF2_), transcription factors, signaling pathways, and DNA damage response genes (eg, _TP53_). Cytogenetic changes, including loss of chromosome 5q [del(5q)], 7q, monosomy 7, and trisomy 8, among others, are found in >50% of cases of MDS.[5] At diagnosis, patients often harbor

several of these abnormalities, making it difficult to reconstruct trajectories of somatic evolution. As a result, the order in which genetic changes are acquired and their functional consequences on hematopoietic stem and progenitor cell (HPC) self-renewal and differentiation remain incompletely understood.

The order of acquisition of pathogenic mutations has a profound clinical impact.[6] Several strategies have been used to identify and order clonal events. Whole-genome or whole-exome sequencing (WGS/WES) has been extensively used to track and quantify disease alleles.[7,8] Although WGS does not inform clonal history of mutations, it can be inferred by correlating mutant allele frequencies. WGS is not informative, however, if mutations are rare or fully clonal, typified by early disease mutations shared by all malignant cells. Tracking mutant alleles over multiple longitudinal samples from the same patient can help resolve patterns of clonal progression,[9] although in most clinical cases, only a single patient sample is available. Mutations found in CH, most commonly _DNMT3A_, _TET2_, and _ASXL1_, are predicted to

be disease-initiating.[10] However, these mutations are not found in some patients, whereas multiple CH-associated mutations can occur in others. Single-cell methods enable more direct assessment of clonal composition.[11] However, because early subclones are outcompeted by more malignant descendants, they may be rare and difficult to detect directly. More fundamentally, current approaches do not enable both molecular identification and a functional assessment of individual cells, making it difficult to study how acquisition of mutations affects HPC self-renewal, differentiation, and response to treatment.

Yamanaka factors Oct4, Sox2, Klf4, and Myc (OSKM) reprogram a somatic cell into an induced pluripotent stem cell (iPSC), which retains the somatic cell genome, including any somatic mutations.[12] iPSC colonies thus capture somatic genomes of single cells, providing a sampling of cellular heterogeneity. iPSCs can be clonally expanded and differentiated into HPCs, enabling direct functional assessment of individual subclones.[13] Individual mutations can be gene corrected, enabling interrogation of their causative role. Thus, reprogramming enables molecular and functional interrogation of single patient cells.

Cancer cells can be reprogrammed to pluripotency and retain tumorigenic potential upon differentiation.[14,15] More recently, MDS and acute myeloid leukemia (AML) patient samples have been reprogrammed, although in most cases a single subclone was captured from each patient.[16,17] In one notable case, KRAS wild-type and mutant subclones were reprogrammed from a patient with AML exhibiting outgrowth of the wild-type allele during relapse.[17] Samples from patients with more advanced MDS showed decreased efficiency of differentiation to HPCs corresponding to a progressive block in differentiation.[16] However, it has been challenging to generate isogenic iPSC lines harboring different oncogenic mutations to provide insights into mechanisms of disease evolution.

Here we show that episomal reprogramming of MDS patient samples generates iPSCs from rare preleukemic cells with a partial complement of mutations, informing somatic mutation order in individual patients. Reprogramming identified the earliest clonal intermediates, which were rarely detected among single patient cells. We used this strategy to establish the order of mutations and gain insight into how sequential acquisition of mutations contributes to disease. We show that mutations in SF3B1 found in ~20% of MDS[18] could occur as a second hit that perturbed mitochondrial function and erythroid differentiation. In a patient with MDS with complex karyotype, we identified del(5q) as an early cytogenetic lesion that perturbed genome stability and differentiation. The current study illustrates the broad utility of reprogramming in understanding leukemic progression.

Methods

Patient samples and reprogramming

Bone marrow and peripheral blood mononuclear cells were obtained from patients according to the institutional guidelines approved by the University of Washington and Fred Hutchinson Cancer Center Institutional Review Board. A complete list of samples is listed in supplemental Table 1 (available on the *Blood* Web site). For Sendai, cells were reprogrammed by using the

Cytotune iPS Sendai Reprogramming Kit (Thermo Fisher Scientific) following the manufacturer's instructions. The episomal reprogramming protocol was developed based on the methods of Okita et al[19] and is detailed in the supplemental Methods.

iPSC culture

iPSCs were maintained on Matrigel (BD) in mTeSR1 (StemCell Technologies) medium. Medium was changed daily, and cells were passaged in a 1:10 ratio every 5 to 7 days by using standard passaging techniques with Dispase (StemCell Technologies). Before differentiation, colonies were passaged for one passage onto CF-1 mouse embryonic fibroblasts in human embryonic stem cell medium: Dulbecco's modified Eagle medium (DMEM)/F12 + 20% KnockOut-Serum Replacement (Invitrogen), 1 mM L-glutamine, 1 mM nonessential amino acid, 0.1 mM β-mercaptoethanol, and 10 ng/mL basic fibroblast growth factor (PeproTech). CF-1 mouse embryonic fibroblasts were prepared by inactivation with 0.5 mg/mL mitomycin C for 2 hours before cryopreservation.

Embryoid body differentiation

iPSCs were scraped into nonadherent rotating 10 cm plates with KnockOut-DMEM + 20% fetal bovine serum (FBS), 1 mM L-glutamine, 1 mM nonessential amino acid, P/S, 0.1 mM β-mercaptoethanol, 200 μg/mL h-transferrin, and 50 μg/mL ascorbic acid. After 24 hours, medium was changed by allowing embryoid bodies (EBs) to settle by gravity and replaced with EB medium plus growth factors: 50 ng/mL BMP4 (R&D Systems), 100 ng/mL stem cell factor (SCF), 100 ng/mL FLT3, 10 ng/mL granulocyte colony-stimulating factor, 20 ng/mL interleukin-6 (IL-6), and 10 ng/mL IL-3 (PeproTech). Medium was changed on days 5 and 10. EBs were dissociated on day 14 with collagenase B (Roche), followed by enzyme-free dissociation buffer (Gibco), and filtered through an 80 μm filter. EBs were frozen in 10% dimethyl sulfoxide, 40% FBS freezing solution.

EB progenitor sorting

Dissociated EB cells were thawed by using the Lonza Poietics protocol and resuspended at 1×10^6/100 μL staining buffer (phosphate-buffered saline + 2% FBS). Cells were stained with a 1:50 dilution of CD45 APC (HI30), CD34 PE (8G12), CD43 PerCP-Cy5.5 (1G10) (all BD Biosciences), and 4′,6-diamidino-2-phenylindole for 20 minutes at room temperature. All sorting was performed on a BD FACS Aria II cell sorter using a 70 μm nozzle.

5F gene transfer and CD34-5F culture

Sorted CD34+CD45+ EB progenitors were seeded on RetroNectin-coated (10 μg/cm²) 96 well plates at a density of 2 to 5×10^4 cells per well. The infection medium was StemSpan SFEM (StemCell Technologies) with 50 ng/mL SCF, 50 ng/mL FLT3, 50 ng/mL thrombopoietin (TPO), 50 ng/mL IL-6, and 10 ng/mL IL-3. Lentiviral infections were performed in a total volume of 150 μL. The multiplicity of infection (MOI) for the factors was MOI = 5 for ERG and HOXA9, and MOI = 3 for RORA, SOX4, and MYB. Virus was concentrated onto cells by centrifuging the plate at 2500 rpm for 30 minutes at room temperature. Infections were performed for 24 hours. After gene transfer, CD34-5F cells were cultured in SFEM with 50 ng/mL SCF, 50 ng/mL FLT3, 50 ng/mL TPO, 50 ng/mL IL-6, and 10 ng/mL IL-3 (PeproTech). Doxycycline (Dox) was added at 2 μg/mL (MilliporeSigma). Cultures were maintained at $<1 \times 10^6$ cells/mL and medium changed

every 3 to 4 days. CD34-5F lines were routinely cultured between 21 and 100 days and maintained normal karyotype and differentiation potential.

Erythroid differentiation

Differentiation was performed as previously described.[20] The complete protocol is given in the supplemental Methods. Perls' Prussian blue staining was performed by using the Iron Stain kit (MilliporeSigma).

Flow cytometry

Erythroid differentiation was analyzed by using CD71 APC-H7 (M-A712; BD) and CD235a/Glycophorin A PE-Cy7 (11E4B-7-6; Beckman Coulter). Staining was performed with $<5 \times 10^5$ cells per 100 μL staining buffer (phosphate-buffered saline + 2% FBS) with 1:50 dilution of each antibody, 20 minutes at room temperature in dark. For Mitotracker staining, cells were stained with 200 nM Mitotracker Green (MTG) and 100 nM TMRE (Molecular Probes) together with CD71 and CD235a in 200 μL Iscove modified Dulbecco medium for 20 minutes at 37°C. For annexin V, cells were washed in staining buffer and resuspended in 1:50 of annexin V-APC in the annexin staining buffer (BD Biosciences) for 20 minutes at room temperature. Fluorescence minus one was used to set flow cytometer settings. Acquisition was performed on BD LSRII.

Colony assays

MDS patient bone marrow mononuclear cells (BMMCs) were enriched for HPCs by using CD34+ beads (Miltenyi) and plated at 1000, 2500, or 5000 cells/mL in 3 mL MethoCult (H3434; StemCell Technologies), plus 10 ng/mL FLT3, 10 ng/mL IL-6, and 50 ng/mL TPO. CD34-5F cells were plated at 1×10^4 or 5×10^4 cells/mL. Mixture was distributed into two 60 mm dishes and maintained in a humidified chamber for 14 days.

Statistical analysis

Statistical analysis was performed with GraphPad Prism software. Data are shown as the mean with standard deviation from the mean unless noted. Pairwise comparisons between groups were performed by using a 2-sided unpaired unequal variance t test unless otherwise noted. For all analyses, $P < .05$ was considered statistically significant. Investigators were not blinded to the different groups.

Results

Reprogramming identifies stages of clonal evolution in MDS

Patients with MDS often harbor multiple mutations and cytogenetic lesions, making it difficult to establish patterns of clonal evolution. Because preleukemic cells may persist long after disease onset,[2] we reasoned that reprogramming can generate iPSC lines from clonal intermediates (Figure 1A). To test this theory, we reprogrammed a patient with MDS with isolated del(5q) and refractory anemia (MDS-RA1) (supplemental Table 1). Karyotyping identified a reciprocal translocation between chromosomes 4 and 12 [t(4;12)] in 38 of 40 cells and a del(5q) in 86.5% of cells by fluorescence in situ hybridization (FISH) (Figure 1B-C). Targeted sequencing of commonly mutated MDS and AML genes identified heterozygous missense mutations in SF3B1 (p.G742D, variant allele fraction [VAF] 36%) and

EZH2 (p.R685H, VAF 43%). SF3B1 is recurrently mutated in MDS with ring sideroblasts (MDS-RS).[21,22] All 4 clonal abnormalities in this patient were present in the majority of MDS cells, making it impossible to assign mutational order given a single bone marrow aspirate.

To determine if discrete stages of preleukemic clonal evolution marked by these 4 clonal abnormalities could be identified, we reprogrammed CD34+ progenitors isolated from BMMCs to pluripotency using Sendai virus, a high-efficiency and nonintegrating method. iPSC colonies positive for pluripotency markers Tra-160 and SSEA-4 were isolated and genotyped by allele-specific polymerase chain reaction and Sanger sequencing, or cytogenetic abnormalities by karyotype, FISH, and single nucleotide polymorphism (SNP) genome arrays. Three (16%) of 19 iPSC colonies were positive for the SF3B1 and EZH2 mutations and the patient-specific cytogenetic change, t(4;12) but not del(5q), indicating that the 3 colonies derived from the same MDS subclone (Sendai) (Figure 1D). The remaining 16 colonies lacked clonal abnormalities and were thus likely derived from normal CD34+ progenitors.

As a second approach, given the low efficiency of reprogramming MDS cells, we performed episomal transfection of CD34+ progenitors, which has a lower efficiency of reprogramming normal cells compared with Sendai.[19] By contrast, MDS cells were more efficiently reprogrammed by episomes, with 13 (72%) of 18 Tra-160 and SSEA-4–positive iPSC colonies harboring patient-specific abnormalities, consistent with the frequency of mutant cells in the patient sample (episomal) (Figure 1D). Episomal reprogramming had a higher efficiency of reprogramming MDS cells compared with Sendai in 2 other patients with MDS (supplemental Figure 1A). MDS-iPSCs grouped into 4 genetically distinct sets corresponding to subclones in the patient (Figure 1E). All 13 MDS-derived iPSCs harbored t(4;12)(q31.3; q15), suggesting it was the initial abnormality. Of these 13 lines, 11 had t(4;12) and the SF3B1 mutation but not the EZH2 or del(5q), suggesting that SF3B1 occurred second. Seven iPSC lines had t(4;12), SF3B1, and EZH2 mutations but not del(5q). Two of 13 lines had the full complement of patient-specific abnormalities, including del(5q). Based on this pattern, the most parsimonious explanation is that t(4;12) was the initiating event, followed by mutations in SF3B1, EZH2, and del(5q), in that order (Figure 1E-F).

To exclude the possibility of gene conversion to wild-type alleles, we monitored heterozygosity at nearby SNPs. The closest EZH2 intronic SNP rs740949 C/T (378 bp) remained heterozygous in all iPSCs (supplemental Figure 1B). None of the lines harbored karyotypic abnormalities other than t(4;12)(q31.3; q15), indicating that no abnormalities were acquired during reprogramming (supplemental Figure 1C). SNP arrays confirmed copy number loss at 5q31.2 (supplemental Figure 1D) but showed no other regions of copy number variations or loss of heterozygosity (LOH) due to uniparental disomy in any of the iPSC lines (supplemental Figure 1E). Targeted sequencing did not identify de novo oncogenic mutations in patient iPSCs (supplemental Table 2). These data indicate that reprogramming faithfully captured the patient's MDS genomes.

Exome sequencing identified 12 somatic variants in the patient acquired during disease evolution (supplemental Table 3). Of

these, 2 (*PLXNB1* and *RBM19*) were present in t(4;12)-only iPSCs, 9 in t(4;12);SF3B1 iPSCs (*SF3B1*, *NAALAD2*, *TTYH2*, *NFE2*, *USH2A*, *DCHS1*, and *LMAN1L*), and 12 in t(4;12);SF3B1;EZH2 iPSCs (*EZH2*, *PSPC1*, and *ZFHX4*) (Figure 1F). In addition, we reproducibly generated iPSCs from clonal intermediates in other MDS subtypes and conducted WES to map somatic evolution (supplemental Figure 2; supplemental Table 4). Thus, reprogramming is a broadly applicable strategy to order somatic variants during preleukemic clonal evolution.

To compare subclonal representation in iPSCs to single cells, we isolated colonies (colony-forming units [CFUs]) derived from single patient CD34+ cells previously shown to inform mutational order[6] and genotyped for t(4;12), *SF3B1*, *EZH2*, and del(5q). Most colonies were derived from either normal cells (34%) or MDS cells with all 4 abnormalities (56%) (Figure 1G). Only 3 (5%) of 62 colonies were clonal intermediates negative for del(5q), and 3 (5%) of 62 were negative for del(5q) and *EZH2*. None of the colonies (of 62) had a single mutation, making it impossible to discriminate between t(4;12) and *SF3B1* as the initiating mutation. Premalignant intermediates are thus rare among single cells but preferentially captured in reprogramming, whereas cells with multiple oncogenic events are reprogrammed less efficiently. Preferential reprogramming of preleukemic subclones was observed across multiple MDS patient samples, especially with cytogenetic anomalies (Figure 1H). Altogether, reprogramming uniquely resolves the order of disease-initiating mutations by capturing preleukemic cells within a single MDS patient sample.

Disease progression impairs hematopoietic differentiation

Subclonal MDS-iPSC lines can be used to investigate how sequential acquisition of mutations contributes to disease progression. To study the functional impact of somatic evolution in an individual patient, we differentiated normal, t(4;12), t(4;12);SF3B1, t(4;12);SF3B1;EZH2, and t(4;12);SF3B1;EZH2; del(5q) iPSCs from an MDS-RA1 patient to HPCs by using a 14-day EB protocol. Isogenic wild-type iPSCs gave rise to 83.4 ± 5.24% CD45+ hematopoietic cells, of which about one-half were CD34+CD45+ HPCs (Figure 2A). Leukemic progression is associated with reduced efficiency of hematopoietic differentiation.[16] Hematopoietic differentiation was only modestly reduced by the initiating t(4;12) translocation (76.8 ± 3.51%), suggesting that it may have promoted clonal expansion but did not perturb differentiation in this assay (Figure 2A-B). By contrast, *SF3B1*-mutant iPSCs representing the second pathogenic hit showed markedly decreased differentiation efficiency (28.0 ± 4.80% CD45+; *P* < .001), which was further reduced upon disease progression to the t(4;12);SF3B1;EZH2 subclone (11.4 ± 1.57% CD45+; *P* < .001). Clonal evolution in this patient is thus mirrored by a progressive decline in efficiency of hematopoietic differentiation.

We next sought to determine whether the decreased hematopoietic differentiation of MDS iPSCs is due to altered proliferation or apoptosis of HPCs, or inefficient development of HPCs. Cell cycle progression marked by 5-ethynyl-2′-deoxyuridine (EdU) incorporation was unchanged in HPCs derived from all 5 isogenic iPSC lines (Figure 2C). Apoptosis was not affected by the *SF3B1* mutation and modestly but not significantly

increased in *EZH2*-mutant HPCs (Figure 2D). We next examined the earlier wave of hematopoiesis marked by CD43, which develops independently from hemogenic endothelium.[23] Clonal evolution was mirrored by a progressive decline in CD43+ hematopoiesis (supplemental Figure 3A-B). These data suggest that somatic mutations do not affect proliferation or apoptosis of iPSC-derived HPCs but likely impair hematopoietic development from earlier precursors.

Acquisition of the *SF3B1* mutation marked a pronounced effect on differentiation. To determine the role of *SF3B1*, we abolished the mutant p.G742D allele in t(4;12);SF3B1;EZH2 Sendai iPSCs by introducing an upstream 1 bp deletion (p.G740fs, NM_012433.2: c.2219delG), resulting in a stop codon at position 747, by CRISPR/Cas9. p.G742D-ablated iPSCs (-G742D) showed a partial rescue of hematopoietic differentiation (25.4% CD45+ cells) compared with Cas9-transfected but uncorrected *SF3B1*-mutant cells (10.1% CD45+ cells; *P* = .02) (Figure 2E). The acquisition of the *SF3B1* mutation was thus a key pathogenic event in early disease evolution that perturbed HPC differentiation.

SF3B1 causes mitochondrial dysfunction

SF3B1 mutations in MDS are associated with mitochondrial iron sequestration and ineffective erythropoiesis.[24] *EZH2* and *SF3B1* comutations are associated with more severe anemia and transfusion dependence in MDS-RS.[22] To define the basis by which these mutations perturb erythropoiesis, we differentiated CD34+CD43+ HPCs from subclonal iPSCs to CD71+CD235a+ erythroid cells. Acquisition of mutations progressively impaired erythroid differentiation (supplemental Figure 3A,C), accompanied by increased apoptosis, a hallmark of ineffective erythropoiesis (supplemental Figure 3A,D). However, low numbers of MDS HPCs derived by direct differentiation precluded more detailed characterization.

To overcome this limitation, we expanded CD34+CD45+ day 14 HPCs by Dox-dependent expression of 5 transcription factors (CD34-5F). Erythroid differentiation is initiated by removing Dox and follows the same stages as primary CD34+ cells.[25] CD34-5F cells derived from t(4;12);SF3B1, and t(4;12);SF3B1;EZH2 patient iPSCs gave rise to slightly more CD71+CD235a+ erythroblasts compared with isogenic control cells but had decreased efficiency of CD71loCD235a+ terminal maturation (Figure 3A). Prussian blue iron staining of MDS-derived erythroid precursors visualized some sideroblasts meeting morphologic criteria for ring sideroblasts (minimum of 5 granules encircling at least one-third of the circumference of the nucleus[26]), which were absent in erythroid culture of normal isogenic cells (Figure 3B). At day 11 of differentiation, 42.3% of t(4;12);SF3B1;EZH2 erythroblasts stained positive for annexin V, a marker of apoptosis, compared with 11.6% of t(4;12);SF3B1 and 7.6% of isogenic control cells (Figure 3C). CRISPR/Cas9-mediated ablation of the *SF3B1* p.G742D allele or enforced expression of EZH2 partially decreased the frequency of apoptotic cells (supplemental Figure 3E), suggesting that *SF3B1* and *EZH2* mutations cooperate to induce apoptosis. *SF3B1*-mutant iPSCs thus display ineffective erythropoiesis marked by iron sequestration and apoptosis, consistent with previous reports with MDS-RS patient cells.[27]

We next investigated if ineffective erythropoiesis is due to mitochondrial dysfunction by co-staining with tetramethylrhodamine (TMRE), which marks metabolically active mitochondria, and
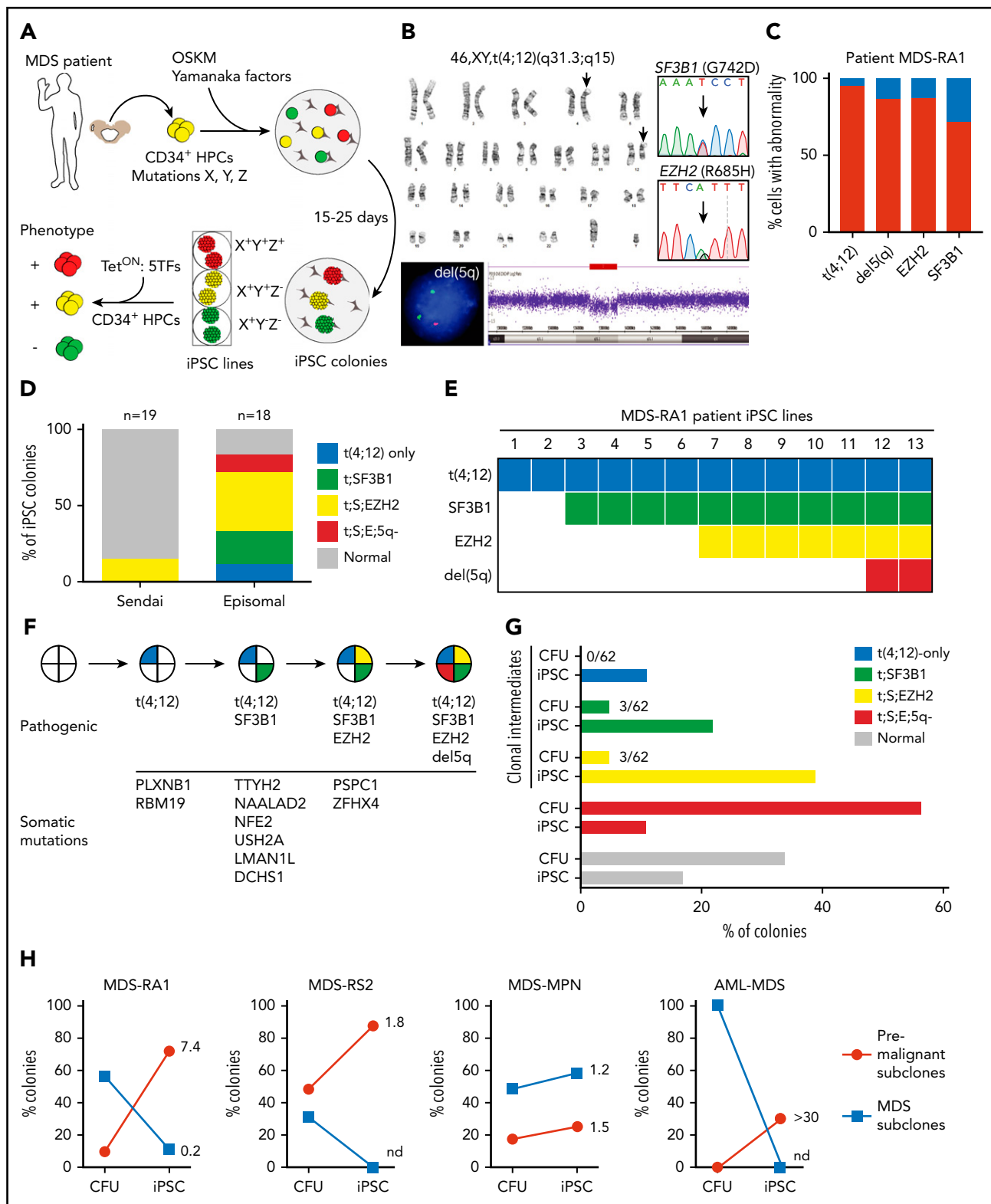
Figure 1. Reprogramming identifies stages of clonal evolution in MDS. (A) Experimental scheme. BMMCs are extracted from the iliac crest of patients with MDS and cryopreserved. CD34$^+$ HPCs are isolated and reprogrammed by episomal transfection of OSKM transcription factors. Single reprogrammed cells give rise to iPSC colonies, and individual colonies are genotyped for disease alleles and expanded into clonal iPSC lines. Individual lines are differentiated into CD34$^+$ HPCs and multipotential progenitor lines established by 5F transfection. (B) Molecular abnormalities present in the MDS-RA1 patient. Standard karyotype showing the reciprocal t(4;12)(q31.3;q15) translocation (arrows). EGR1(red)/D5S23 FISH and SNP arrays showing a del(5q)(q31.2) deletion; and Sanger sequencing showing heterozygous *EZH2* (p.R685H, NM_001203247.1: c.2054G>A) and *SF3B1* (p.G742D, NM_012433.2: c.2225G>A) mutations. (C) Percentage of patient BMMCs positive for t(4;12) by karyotyping, del(5q) by FISH, and point mutations (VAF × 2 for heterozygous mutations). (D) Genotyping of iPSC lines generated by nonintegrating Sendai or episomal reprogramming. iPSC lines were genotyped for t(4;12) by karyotyping, del(5q) by FISH, and Sanger sequencing for point mutations. Percent iPSCs of each genotype is indicated by color (total isolated = n), with gray indicating colonies negative for
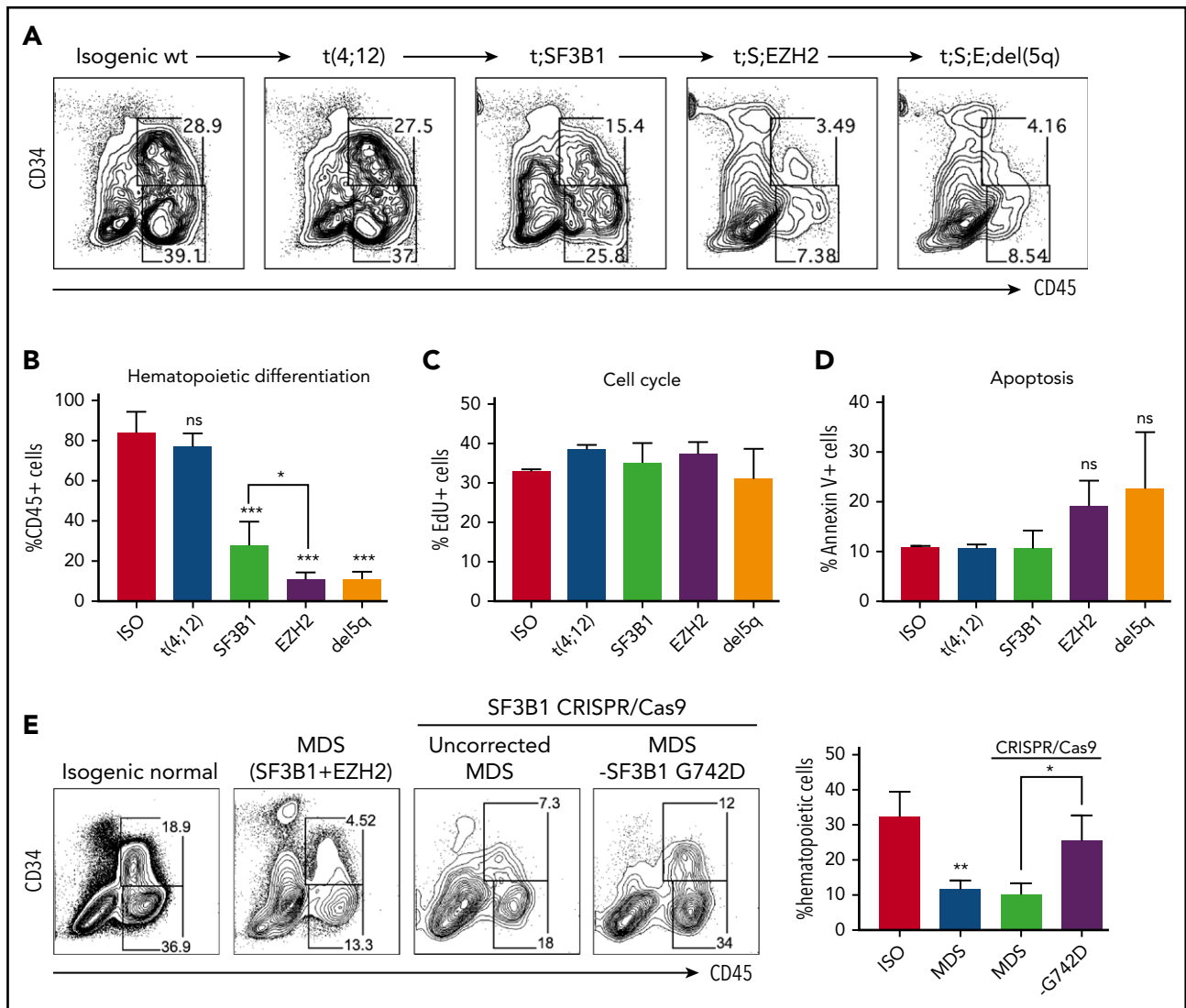
Figure 2. Disease progression impairs hematopoietic differentiation. Hematopoietic differentiation (day 14) of isogenic MDS-RA1 patient iPSCs showing representative flow plots (A) and percentage of CD45$^+$ hematopoietic cells for each genotype (B): normal (ISO), t(4;12), t(4;12);SF3B1 (t;SF3B1), t(4;12);SF3B1;EZH2 (t;S;EZH2), and t(4;12);SF3B1;EZH2; del(5q) (t;S;E;del5q). (B) Mean ± standard deviation (SD) of 2 to 3 iPSCs per genotype, 4 independent experiments. (C) Percentage of EdU-positive actively cycling CD34$^+$CD45$^+$ isogenic HPCs after 3 hours of EdU labeling. (D) Percentage of annexin V$^+$ apoptotic CD34$^+$CD45$^+$ HPCs. (C-D) Mean ± SD of 1 iPSC line per genotype, 3 independent experiments. (E) Hematopoietic differentiation efficiency (%CD45$^+$ cells) of normal (ISO) and t(4;12);SF3B1;EZH2 (MDS) iPSCs generated by using Sendai reprogramming. *SF3B1* p.G742D-ablated (p.G740fs, NM_012433.2: c.2219delG) labeled "-G742D," and noncorrected *SF3B1*-mutant iPSCs, were generated by using CRISPR/Cas9. Quantitation is shown as mean ± SD of 2 independent iPSCs, 2 to 3 independent experiments. For all panels, ***$P < $.001, **$P < $.005, *$P < $.05; unpaired t test vs normal isogenic iPSCs unless indicated. ns, not significant.

Mitotracker Green (MTG), which marks mitochondria irrespective of activity. *SF3B1*-mutant erythroblasts had similar levels of TMRE-positive mitochondria but increased MTG-positive mitochondria compared with isogenic control (Figure 3D). A decreased TMRE:MTG ratio is indicative of metabolically inactive or damaged mitochondria. The levels of MTG-positive mitochondria increased during disease progression in the patient from normal isogenic to t(4;12);SF3B1 (1.31-fold; $P = $.08), to t(4;12);SF3B1;EZH2 (1.78-fold; $P = $.0001) cells, and were reduced by genetically ablating the *SF3B1* p.G742D allele (Figure 3E). Consistent with this action, the TMRE:MTG ratio decreased during disease progression from normal isogenic (0.65) to t(4;12);SF3B1 (0.47; $P = $.1), to t(4;12);SF3B1;EZH2 (0.34; $P = $.01) cells, and was rescued by ablation of the *SF3B1*

Figure 1 (continued) MDS mutations. Genotypes are abbreviated as follows: t(4;12)-only, t(4;12);SF3B1 (t;SF3B1), t(4;12);SF3B1;EZH2 (t;S;EZH2), t(4;12);SF3B1;EZH2;del(5q) (t;S;E; 5q). (E) Genotypes of the individual iPSC lines (across) showing successive acquisition of patient-specific abnormalities (down). Only MDS-derived iPSCs are shown. (F) The inferred order of somatic mutations during clonal evolution. Somatic variants were identified by WES in the patient and one or more subclonal MDS-iPSCs but not in normal isogenic iPSCs. Variants are ordered according to iPSC genotype. Complete data are shown in supplemental Table 3. (G) Comparison of clonal representation (percentage of total colonies) by genotyping CFUs (n = 62) and iPSCs derived from patient CD34$^+$ cells. Single colonies were genotyped for each mutation by allele-specific quantitative polymerase chain reaction. (H) Proportion of premalignant (red; partial complement of mutations) and malignant (blue; all mutations) subclones in CFU versus iPSC colonies of 4 patients with MDS. Number indicates fold enrichment in iPSCs compared with CFUs.
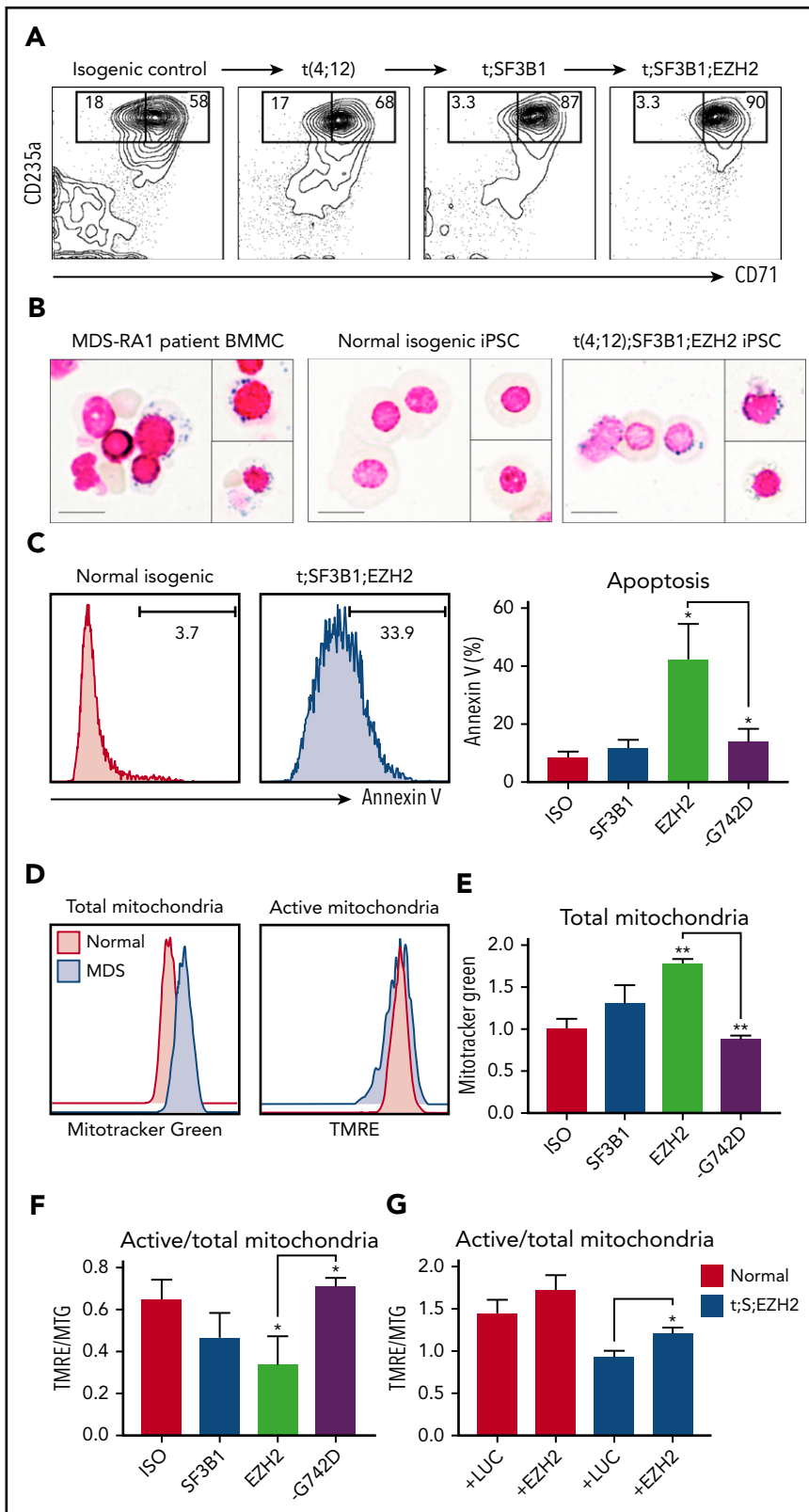
Figure 3. *SF3B1* mutations perturb mitochondrial function. For all panels, isogenic iPSCs are abbreviated: normal (ISO), t(4;12);SF3B1 (t;SF3B1 or SF3B1), t(4;12); SF3B1;EZH2 (t;SF3B1;EZH2 or EZH2), and SF3B1 G742D-ablated (-G742D). (A) Erythroid differentiation of CD34-5F cells derived from MDS-RA1 patient iPSCs. Percentage of early (CD71$^+$CD235a$^+$) and mature (CD71^{lo}CD235a$^+$) erythroblasts, day 11 of differentiation. (B) Prussian blue iron staining of primary BMMCs from patient MDS-RA1 and erythroblasts from normal isogenic or t;SF3B1; EZH2 MDS-iPSCs. Ring sideroblasts were evaluated based on the criteria of >5 iron granules encircling at least one-third of the circumference of the nucleus. Scale bars 15 μm. (C) Frequency of annexin V$^+$ apoptotic CD235a$^+$ erythroid cells derived from isogenic iPSCs. (D) Total and active mitochondrial content in CD235a$^+$ erythroid cells derived from isogenic iPSCs. (E) Total mitochondrial content measured as mean fluorescence intensity (MFI) of MTG in CD235a$^+$ erythroid cells derived from isogenic iPSCs. (F) Ratio of active (measured as MFI of TMRE) to total (measured as MFI of MTG) mitochondria in CD235a$^+$ cells derived from isogenic iPSCs. (G) Ratio of active to total mitochondria in normal (ISO) and t;SF3B1;EZH2 CD235a$^+$ cells transduced with a control luciferase (+LUC) or EZH2 overexpression lentivirus (+EZH2). (C-G) Mean ± standard deviation of 3 experiments, 1 to 2 iPSCs per genotype. **P < .01, *P < .05, t test vs ISO unless indicated.

p.G742D allele (0.71; P = .04) (Figure 3F). These data suggest that mutant *SF3B1* causes mitochondrial dysfunction in the context of cooperating mutations. Because *EZH2* R685H is a predicted loss-of-function mutation, we performed EZH2 overexpression. EZH2 increased the TMRE:MTG ratio in t(4;12);SF3B1;EZH2 erythroid cells (Figure 3G), suggesting that it cooperates with mutant SF3B1. Damaged mitochondria are a source of reactive oxygen species (ROS), which can trigger apoptosis, and we detected a modest increase in ROS levels with the DCFDA dye (supplemental Figure 3F). These findings

identify mitochondrial quality as a target of cooperating mutations in MDS-RS promoting generation of ROS and apoptosis, resulting in ineffective erythropoiesis.

SF3B1 mutations can occur as a second hit

SF3B1 mutations are found in CH and are generally believed to be disease-initiating.[22,27,28] However, in our MDS-RA1 patient, *SF3B1* was the second pathogenic event (Figure 1F). To better define the order of *SF3B1* mutations, we performed reprogramming of 4 additional *SF3B1*-mutant MDS samples with known pathogenic comutations and normal cytogenetics (supplemental Table 1). Three patients had MDS-RS with comutations in *DNMT3A* (p.R882H and p.R635W) or *ASXL1* (p.R417*), and 1 patient had MDS with excess blasts with *RUNX1* (p.P332fs) mutation. Reprogramming identified single-mutant iPSCs in 3 of 4 patients with initiating mutations in *DNMT3A* (MDS-RS1), *ASXL1* (MDS-RS2), and *RUNX1* (MDS with excess blasts) (supplemental Figure 4A). No single-mutant iPSCs were isolated in MDS-RS3 precluding determination of the order. All iPSCs maintained heterozygosity at *SF3B1* intronic SNPs ruling out gene conversion (supplemental Figure 4B). These findings show that in all 4 patients in whom the order of mutations could be experimentally defined, *SF3B1* was the second pathogenic mutation (supplemental Figure 4C), indicating that in some cases, *SF3B1* is a cooperating rather than initiating hit.

Clonal evolution in MDS with complex karyotype

Because cells with multiple oncogenic mutations are generally reprogrammed less efficiently, we next investigated if reprogramming could identify preleukemic evolution in samples with more significant aneuploidy. Complex karyotype (≥3 chromosomal anomalies) is found in 15% to 20% of MDS and associated with *TP53* mutations and poor prognosis.[29,30] We first reprogrammed an AML with MDS-related changes, complex karyotype, with *TP53* and *TET2* mutations. SNP arrays showed multiple copy number losses and gains also seen in the karyotype, including del 1p, −3, del 5(q13-q31), add 8, add 9, add 12, −16, −18, add 19, and +22, and LOH of the *TP53* locus on chromosome 17p13 (Figure 4A; supplemental Figure 5A). After reprogramming, 3 of 10 iPSCs were heterozygous for *TP53* Y220C mutation (Figure 4A-B) but surprisingly had normal karyotype (supplemental Figure 5B) and no structural copy number variations by SNP arrays, indicating that they were derived from preleukemic cells before LOH. By contrast, all (40 of 40) CFUs derived from single CD34+ cells were *TP53*−/− homozygous mutant (Figure 4C), suggesting that *TP53*+/− preleukemic cells are rare but selected during reprogramming. These data suggest that complex karyotype is a barrier to reprogramming, enabling identification of rare preleukemic cells.

The second patient had Li-Fraumeni syndrome with germline *TP53* p.R209fs mutation and developed MDS with complex karyotype (supplemental Table 1). All iPSC lines (n = 12) harbored *TP53* R209fs but similarly had normal 46,XX karyotype that was maintained during passaging (Figure 4D; supplemental Figure5C). Notably, 2 of 12 iPSCs harbored an isolated del(5)(q22-31.1) that was present in the patient but not as an isolated abnormality (Figure 4D-E). SNP arrays confirmed that del(5q) was the only structural abnormality in these iPSCs, and no structural abnormalities were found in the other iPSCs from this patient (supplemental Figure 5D). Thus, del(5q) is an early cytogenetic anomaly associated with *TP53*-mutant MDS.

Del(5q) perturbs hematopoietic differentiation

As an isolated cytogenetic abnormality in MDS, del(5q) is associated with the 5q− syndrome characterized by macrocytic anemia and good prognosis.[31] The 5q22-31.1 deletion in our patient represents a common deleted region in poor-prognosis MDS or AML associated with complex karyotype, in which it specifies poor outcome.[32,33] The significance of del(5q) in poor-prognosis MDS has not been investigated. To identify the role of del(5q), we differentiated TP53+/− Li-Fraumeni and TP53+/−; del(5q) iPSCs to HPCs. Hematopoietic differentiation was reduced in del(5q) iPSCs (P = .003) (Figure 5A), whereas CFU potential was comparable to TP53+/− alone (supplemental Figure 6A). We next established CD34-5F progenitor lines and tracked their colony-forming potential. CFU potential of TP53+/− progenitors remained stable over a month of culture (11.3 ± 2.34 CFUs/1000 CD34+ cells), whereas TP53+/−;del(5q) progenitors gradually lost multilineage differentiation over this period (1.64 ± 1.27; P = .001) (Figure 5B; supplemental Figure 6A-B). Both groups formed similar numbers of colonies with Dox (P = .86), indicating that proliferation of undifferentiated cells was not affected). These findings suggest that 5q loss in *TP53*-mutant cells gradually compromises multilineage hematopoietic differentiation.

Del(5q) promotes genome instability

To study the mechanisms by which differentiation was gradually impaired by loss of 5q, we performed RNA sequencing of CD34+ 5F cells. As expected, gene ontology (GO) annotation exhibited significant downregulation of gene expression within the 5q22-31.1 deleted interval, with genes in the 5q31.1 region most significantly downregulated (Figure 5C; supplemental Table 5). GO annotation by molecular function showed that most significant downregulated categories included genes involved in chromosome and sister chromatid cohesion and segregation (Figure 5D). Some of these downregulated genes localize to the 5q-deleted region, including *RAD50*, *CEP120*, *UBE2B*, *SKP1*, and *LMNB1*. Progression to complex karyotype is associated with chromosome instability (CIN).[34] Genes associated with CIN[35] were also significantly downregulated in TP53+/;del(5q) cells. These data suggest that 5q loss decreases expression of genes involved in DNA damage repair and chromosome stability.

We hypothesized that sporadic loss of 5q in *TP53*-mutant cells promotes accumulation of DNA damage and genome instability over time, leading to a block in differentiation and MDS. To examine this theory, we measured γ-H2AX and 53BP1 foci, which mark the sites of double-strand breaks after γ-irradiation, a p53-dependent genotoxic stress. TP53+/−;del(5q) and TP53+/− HPCs had comparable induction of nuclear γ-H2AX and 53BP1 staining 30 minutes after irradiation (Figure 5E; supplemental Figure 6C). However, the repair of double-strand breaks was markedly delayed in del(5q) cells, evidenced by persistent γ-H2AX and 53BP1 staining 5 hours after irradiation. Del(5q) progenitors also had more annexin V+ apoptotic cells at baseline but failed to induce apoptosis in response to irradiation (supplemental Figure 6D). These data suggest that loss of 5q results in persistent DNA damage in *TP53*-mutant HPCs.

Increased double-strand breaks can result in structural abnormalities, such as LOH at the *TP53* locus. To examine if del(5q)
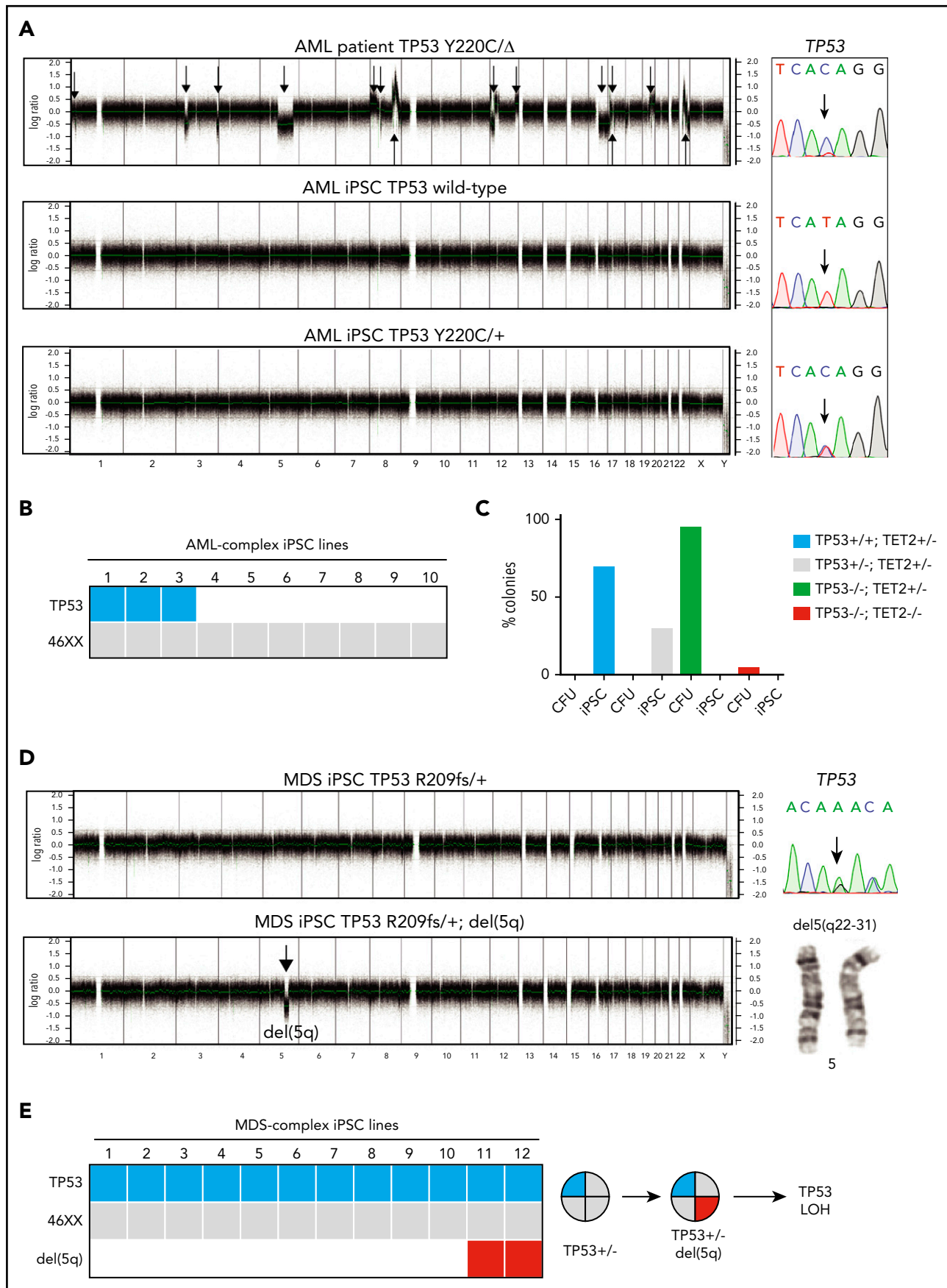
Figure 4.

predisposed to structural abnormalities, we cultured irradiated CD34-5F cells and measured the frequency of *TP53* LOH by using 17p13.1 FISH. Nonirradiated cells maintained a normal karyotype even after extended culture (supplemental Figure 6E). Irradiated TP53^{+/−} cells showed only background frequency of LOH (2.8%), whereas 14% of TP53^{+/−};del(5q) progenitors harbored *TP53* LOH (Figure 5F). These findings suggest that acquisition of del(5q) promotes genome instability, accelerating loss of the second *TP53* allele and progression to complex karyotype.

Discussion

Myeloid neoplasms are preceded by a period of premalignant clonal evolution.[3,4] By the time of diagnosis, malignant cells harbor multiple genetic lesions and continue to evolve in response to treatment, leading to relapse.[36] The nature of disease-initiating events, the order in which they are acquired, and their functional consequences on stem and progenitor cell self-renewal and differentiation remain incompletely understood. We showed that reprogramming of MDS patient samples by using nonintegrating episomal methods generates a panel of iPSC lines that capture the genomes of premalignant clonal intermediates that persist after disease onset.[2,37] Ancestral subclones containing fewer mutations were more likely to be reprogrammed and could be identified even when they were rare among single-patient HPCs. Reprogramming also enables functional analysis of clonal progression by differentiation of iPSCs to HPCs. Previous studies have compared iPSCs from patients at different stages of MDS,[16] complicating direct comparison. By contrast, differentiation of distinct subclones can provide insights into disease progression in individual patients. Using this approach, we identified mitochondrial function and chromosome stability as key pathways affected by acquisition of mutations in MDS.

MDS is a premalignant disorder characterized by aberrant differentiation that has been challenging to model.[4] MDS patient samples are typically cytopenic and engraft poorly in immunodeficient mice.[38] Human cell models have almost exclusively used cell lines that poorly recapitulate human disease. Reprogramming creates versatile disease models that recapitulate aberrant differentiation, dysplastic features, and molecular programs of primary cells.[16,17] However, in most cases, only a single subclone was reprogrammed due to lower efficiency of reprogramming of MDS cells. We find that episomal reprogramming used in this study results in a high proportion of MDS-derived iPSCs, enabling reprogramming of multiple distinct subclones. Because MDS cells have higher levels of innate immune signaling, they may be more prone to apoptosis[39] following infection with Sendai virus, resulting in enrichment for normal cells during reprogramming. In most cases, there was an inverse relationship

between the number of abnormalities, particularly cytogenetic events, and reprogramming efficiency. This scenario favors representation of early preleukemic subclones that may otherwise be too rare to be detected directly. We used this approach to explore mutation order in a small cohort of *SF3B1*-mutant MDS patients. Previous studies have shown that *SF3B1* is usually a founder mutation.[27,28] Our analysis shows that it can be a second hit, preceded by CH-associated epigenetic mutations such as *DNMT3A*, *ASXL1*, and *TET2*. This outcome raises the possibility that *SF3B1* may be either an initiating or a secondary event and that these scenarios might have clinical implications. However, the limited number of patients studied precludes generalization of our conclusions. Our study showed that reprogramming can be used to make important inferences about the order and functional implications of initiating mutations.

To uncover disease-relevant phenotypes, iPSCs must first be differentiated into HPCs. Consistent with previous studies,[16,40] acquisition of mutations in MDS progressively impaired hematopoietic differentiation. We suggest this finding is due to inefficient development of MDS HPCs from hemogenic endothelium, rather than intrinsic defects in proliferation or apoptosis. The limited hematopoietic potential of MDS iPSCs presents a practical challenge for characterizing disease phenotypes.[13] We have adopted a strategy that uses conditional expression of 5 factors to create expandable HPCs.[41] We previously used this system to model congenital anemia and identify therapeutic compounds.[25] The engraftment potential of CD34-5F progenitors remains limited. More recently reported transcription factor protocols may specify more durable engraftment potential.[42] Generation of engraftable MDS HPCs from iPSCs remains an important future goal that would enable modeling of clonal dominance by MDS-HSCs.

Gain-of-function *SF3B1* mutations are strongly associated with MDS-RS,[21,22] suggesting a causative role, but cooperating mutations may also play a role. Unlike other splicing factor mutations, MDS-RS has been challenging to model. An *SF3B1* K700E knock-in mouse model develops anemia but not RS,[43] whereas human knock-in cell lines do not undergo normal erythroid differentiation. By analyzing clonal evolution in a patient with mutant *SF3B1*, we showed that erythroid differentiation is accompanied by iron deposition with findings of ring sideroblasts and accumulation of damaged mitochondria. We propose a model in which rapid mitochondrial biosynthesis combined with iron-induced oxidative damage creates a pool of damaged mitochondria leading to increased ROS and apoptosis. We further showed that mutant *SF3B1* was required and cooperated with *EZH2* mutations to impair mitochondrial function, consistent with more severe anemia in patients with these comutations.[22] Identification of direct targets of SF3B1 that contribute to mitochondrial dysfunction and ring sideroblast formation is a key goal for future study.

Figure 4. Clonal evolution in patients with complex karyotype. (A) SNP genome arrays of AML-MDS patient blasts with complex karyotype and *TP53* (p.Y220C; NM_001126112: c.659A>G) mutation (top). Log signal ratio is plotted. Arrows indicate structural abnormalities. Two representative iPSC lines derived from this patient are shown below, wild-type or heterozygous for the *TP53* Y220C mutation and normal karyotype in the absence of structural abnormalities. (B) Genotypes of individual iPSCs (across) generated from leukemic blasts of the AML patient in panel A. All iPSC lines derived from these patients have a normal 46,XX karyotype. Karyotypes are shown in supplemental Figure 5B. (C) Comparison of clonal composition (as percentage of total colonies) among CD34^{+} cell CFUs (40 colonies) and iPSCs (10 colonies). (D) SNP genome arrays of 2 representative iPSCs reprogrammed from an MDS patient with complex karyotype and an inherited Li-Fraumeni *TP53* (p.R209fs; NM_000546.5: c.626_627del) mutation. Arrow indicates chromosome 5q deletion in one of the iPSC lines. (E) Genotypes of individual iPSCs (across) generated from Li-Fraumeni MDS patient in panel D. All iPSCs derived from these patients have a normal 46,XX karyotype, and 2 lines had an isolated del(5q), one of which is shown in genome view in (D, bottom). Full karyotypes are shown in supplemental Figure 5C.
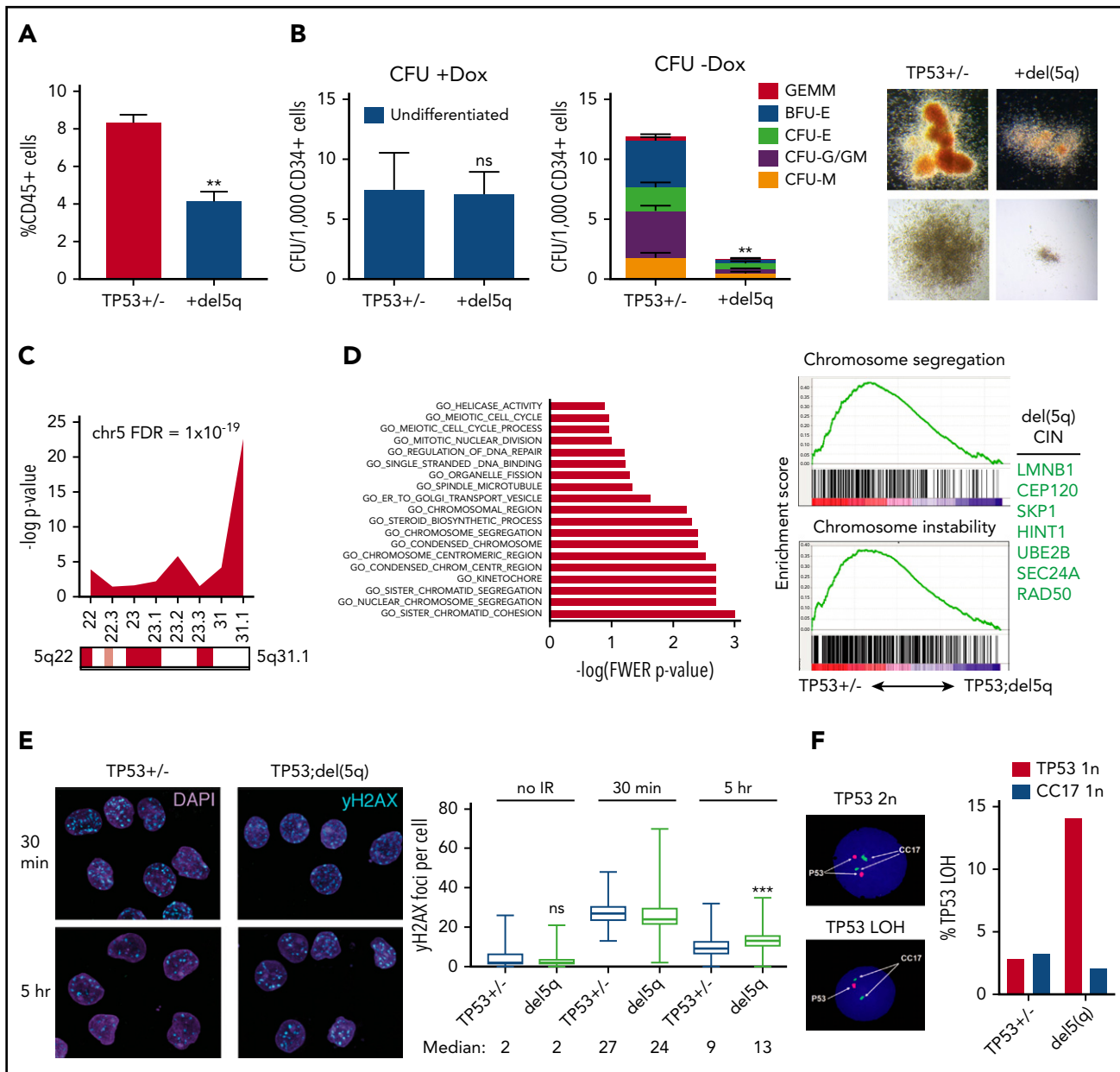
Figure 5. Del(5q) promotes genome instability. (A) Hematopoietic differentiation (%CD45⁺) of isogenic *TP53* R209fs (TP53⁺/⁻) and *TP53* R209fs;del(5q) iPSCs; mean ± standard error of the mean. Two iPSCs per genotype, 2 experiments. **P = .003, *t* test. (B) Colony-forming potential of *TP53* R209fs (TP53⁺/⁻) and *TP53* R209fs;del(5q) CD34⁺5F HPCs. Full dataset is shown in supplemental Figure 6A. Left: undifferentiated CFU (+Dox). Middle: differentiated CFU (–Dox). Right: representative erythroid (BFU-E) and myeloid (CFU-GM) colonies. Two iPSCs per genotype, 2 experiments. **P = .001, *t* test. (C) Chromosomal location of downregulated genes (*P* < .1; 1.5-fold) in del(5q) HPCs. RNA sequencing was performed on *TP53* R209fs (TP53⁺/⁻) and *TP53* R209fs;del(5q) CD34⁺5F cells; *t* test, 2 iPSCs, 2 experiments. (D) Top downregulated GO categories in TP53;del(5q) CD34-5F cells. Left: GO categories ranked by -log of FWER *P* value. Right: gene set enrichment of GO *Chromosome segregation* and *Chromosome instability* gene sets[35] in TP53⁺/⁻ vs TP53;del(5q). Top del(5q) CIN/DDR genes listed. (E) DNA double-strand breaks measured by γ-H2AX foci in CD34⁺5F cells 30 minutes and 5 hours after 4 Gy irradiation. Median ± 95% CI, >100 cells, 2 experiments. ***P < .0001, Mann-Whitney *U* test. (F) Loss of *TP53* heterozygosity detected by 17q FISH in CD34-5F cells cultured for 1 month after 4 Gy of γ-irradiation. CC17, control probe.

Complex karyotype is common in MDS and is associated with *TP53* mutations, del(5q), and poor prognosis.[32,44] Little is known about the mechanisms that lead to genome instability and progression to complex karyotype because chromosomal alterations are difficult to model in mice or engineer into human cell lines. Through our reprogramming method, we identified in one of the patients a del(5q) subclone that preceded evolution to complex karyotype. We find that loss of the 5q22-31.1 region often observed in patients with high-risk MDS and AML dysregulates a gene expression program that maintains genome stability. Del(5q) CD34-5F cells have increased levels of DNA

damage after genotoxic stress and structural loss of *TP53* heterozygosity. This model may thus be instrumental in identifying genes in the 5q-deleted region that maintain chromosomal stability and promote progression to complex karyotypes in MDS and AML.

Our study has shown broad utility of cellular reprogramming to gain insights into clonal evolution during leukemic progression. We anticipate that this approach can be applied broadly to study mechanisms of progression and transformation in hematologic malignancies and cancer.

HSU et al

Acknowledgments

Authorship

Contribution: S.D. and J.L.A. conceived the project; J.H., A.R., J.L.A., and S.D. designed the experiments; J.H., A.R., B.J.H., D.W., and S.D. generated data; J.H., A.R., C.A.C., J.L.A., S.B.K., S.G., D.W., E.Q.K., and S.D. analyzed data; P.S.B., S.B.K., J.L.A., and B.T.-S. provided essential clinical samples and clinical history; and J.H., A.R., J.L.A., S.B.K., and S.D. prepared the manuscript.

Conflict-of-interest disclosure: The authors declare no competing financial interests.

ORCID profiles: E.Q.K., 0000-0001-5904-1788; P.S.B., 0000-0001-6235-9463; S.D., 0000-0002-1328-364X.

Correspondence: Sergei Doulatov, Division of Hematology, Department of Medicine, University of Washington, 1705 NE Pacific St, Box 357710, Seattle, WA 98195; e-mail: doulatov@uw.edu.

Footnotes

REFERENCES

1. Greaves M, Maley CC. Clonal evolution in cancer. *Nature*. 2012;481(7381):306-313.

2. Jan M, Snyder TM, Corces-Zimmerman MR, et al. Clonal evolution of preleukemic hematopoietic stem cells precedes human acute myeloid leukemia. *Sci Transl Med*. 2012;4(149):149ra118.

3. Bowman RL, Busque L, Levine RL. Clonal hematopoiesis and evolution to hematopoietic malignancies. *Cell Stem Cell*. 2018;22(2):157-170.

4. Sperling AS, Gibson CJ, Ebert BL. The genetics of myelodysplastic syndrome: from clonal haematopoiesis to secondary leukaemia. *Nat Rev Cancer*. 2017;17(1):5-19.

5. Haase D. Cytogenetic features in myelodysplastic syndromes. *Ann Hematol*. 2008;87(7):515-526.

6. Ortmann CA, Kent DG, Nangalia J, et al. Effect of mutation order on myeloproliferative neoplasms. *N Engl J Med*. 2015;372(7):601-612.

7. Welch JS, Ley TJ, Link DC, et al. The origin and evolution of mutations in acute myeloid leukemia. *Cell*. 2012;150(2):264-278.

8. Makishima H, Yoshizato T, Yoshida K, et al. Dynamics of clonal evolution in myelodysplastic syndromes. *Nat Genet*. 2017;49(2):204-212.

9. da Silva-Coelho P, Kroeze LI, Yoshida K, et al. Clonal evolution in myelodysplastic syndromes. *Nat Commun*. 2017;8:15099.

10. Jaiswal S, Fontanillas P, Flannick J, et al. Age-related clonal hematopoiesis associated with adverse outcomes. *N Engl J Med*. 2014;371(26):2488-2498.

11. Paguirigan AL, Smith J, Meshinchi S, Carroll M, Maley C, Radich JP. Single-cell genotyping demonstrates complex clonal diversity in acute myeloid leukemia. *Sci Transl Med*. 2015;7(281):281re2.

12. Takahashi K, Tanabe K, Ohnuki M, et al. Induction of pluripotent stem cells from adult human fibroblasts by defined factors. *Cell*. 2007;131(5):861-872.

13. Vo LT, Daley GQ. De novo generation of HSCs from somatic and pluripotent stem cell sources. *Blood*. 2015;125(17):2641-2648.

14. Hochedlinger K, Blelloch R, Brennan C, et al. Reprogramming of a melanoma genome by nuclear transplantation. *Genes Dev*. 2004;18(15):1875-1885.

15. Papapetrou EP. Patient-derived induced pluripotent stem cells in cancer research and precision oncology. *Nat Med*. 2016;22(12):1392-1401.

16. Kotini AG, Chang CJ, Chow A, et al. Stage-specific human induced pluripotent stem cells map the progression of myeloid transformation to transplantable leukemia. *Cell Stem Cell*. 2017;20(3):315-328.e7.

17. Chao MP, Gentles AJ, Chatterjee S, et al. Human AML-iPSCs reacquire leukemic properties after differentiation and model clonal variation of disease. *Cell Stem Cell*. 2017;20(3):329-344.e327.

18. Papaemmanuil E, Gerstung M, Malcovati L, et al; Chronic Myeloid Disorders Working Group of the International Cancer Genome Consortium. Clinical and biological implications of driver mutations in myelodysplastic syndromes. *Blood*. 2013;122(22):3616-3627, quiz 3699.

19. Okita K, Yamakawa T, Matsumura Y, et al. An efficient nonviral method to generate integration-free human-induced pluripotent stem cells from cord blood and peripheral blood cells. *Stem Cells*. 2013;31(3):458-466.

20. Lee HY, Gao X, Barrasa MI, et al. PPAR-α and glucocorticoid receptor synergize to promote erythroid progenitor self-renewal. *Nature*. 2015;522(7557):474-477.

21. Papaemmanuil E, Cazzola M, Boultwood J, et al; Chronic Myeloid Disorders Working Group of the International Cancer Genome Consortium. Somatic SF3B1 mutation in myelodysplasia with ring sideroblasts. *N Engl J Med*. 2011;365(15):1384-1395.

22. Malcovati L, Karimi M, Papaemmanuil E, et al. SF3B1 mutation identifies a distinct subset of myelodysplastic syndrome with ring sideroblasts. *Blood*. 2015;126(2):233-241.

23. Kennedy M, Awong G, Sturgeon CM, et al. T lymphocyte potential marks the emergence of definitive hematopoietic progenitors in human pluripotent stem cell differentiation cultures. *Cell Reports*. 2012;2(6):1722-1735.

24. Malcovati L, Cazzola M. Recent advances in the understanding of myelodysplastic syndromes with ring sideroblasts. *Br J Haematol*. 2016;174(6):847-858.

25. Doulatov S, Vo LT, Macari ER, et al. Drug discovery for Diamond-Blackfan anemia using reprogrammed hematopoietic progenitors. *Sci Transl Med*. 2017;9(376):eaah5645.

26. Mufti GJ, Bennett JM, Goasguen J, et al; International Working Group on Morphology of Myelodysplastic Syndrome. Diagnosis and classification of myelodysplastic syndrome: International Working Group on Morphology of myelodysplastic syndrome (IWGM-MDS) consensus proposals for the definition and

enumeration of myeloblasts and ring side-roblasts. *Haematologica*. 2008;93(11):1712-1717.

27. Mortera-Blanco T, Dimitriou M, Woll PS, et al. *SF3B1*-initiating mutations in MDS-RSs target lymphomyeloid hematopoietic stem cells. *Blood*. 2017;130(7):881-890.

28. Mian SA, Rouault-Pierre K, Smith AE, et al. SF3B1 mutant MDS-initiating cells may arise from the haematopoietic stem cell compartment. *Nat Commun*. 2015;6(1):10004.

29. Wong TN, Ramsingh G, Young AL, et al. Role of TP53 mutations in the origin and evolution of therapy-related acute myeloid leukaemia. *Nature*. 2015;518(7540):552-555.

30. Lindsley RC, Saber W, Mar BG, et al. Prognostic mutations in myelodysplastic syndrome after stem-cell transplantation. *N Engl J Med*. 2017;376(6):536-547.

31. Ebert BL. Molecular dissection of the 5q deletion in myelodysplastic syndrome. *Semin Oncol*. 2011;38(5):621-626.

32. Jädersten M, Saft L, Smith A, et al. TP53 mutations in low-risk myelodysplastic syndromes with del(5q) predict disease progression. *J Clin Oncol*. 2011;29(15):1971-1979.

33. Jerez A, Gondek LP, Jankowska AM, et al. Topography, clinical, and genomic correlates of 5q myeloid malignancies revisited. *J Clin Oncol*. 2012;30(12):1343-1349.

34. Rücker FG, Dolnik A, Blätte TJ, et al. Chromothripsis is linked to *TP53* alteration, cell cycle impairment, and dismal outcome in acute myeloid leukemia with complex karyotype. *Haematologica*. 2018; 103(1):e17-e20.

35. Stirling PC, Bloom MS, Solanki-Patil T, et al. The complete spectrum of yeast chromosome instability genes identifies candidate CIN cancer genes and functional roles for ASTRA complex components. *PLoS Genet*. 2011;7(4):e1002057.

36. Martincorena I, Raine KM, Gerstung M, et al. Universal patterns of selection in cancer and somatic tissues. *Cell*. 2017;171(5):1029-1041.e21.

37. Corces-Zimmerman MR, Hong WJ, Weissman IL, Medeiros BC, Majeti R. Preleukemic mutations in human acute myeloid leukemia affect epigenetic regulators and persist in remission. *Proc Natl Acad Sci USA*. 2014;111(7):2548-2553.

38. Pang WW, Pluvinage JV, Price EA, et al. Hematopoietic stem cell and progenitor cell mechanisms in myelodysplastic syndromes. *Proc Natl Acad Sci U S A*. 2013;110(8):3011-3016.

39. Barreyro L, Chlon TM, Starczynowski DT. Chronic immune response dysregulation in MDS pathogenesis. *Blood*. 2018;132(15):1553-1560.

40. Kotini AG, Chang CJ, Boussaad I, et al. Functional analysis of a chromosomal deletion associated with myelodysplastic syndromes using isogenic human induced pluripotent stem cells. *Nat Biotechnol*. 2015;33(6):646-655.

41. Doulatov S, Vo LT, Chou SS, et al. Induction of multipotential hematopoietic progenitors from human pluripotent stem cells via respecification of lineage-restricted precursors. *Cell Stem Cell*. 2013;13(4):459-470.

42. Vo LT, Kinney MA, Liu X, et al. Regulation of embryonic haematopoietic multipotency by EZH1. *Nature*. 2018;553(7689):506-510.

43. Obeng EA, Chappell RJ, Seiler M, et al. Physiologic expression of Sf3b1(K700E) causes impaired erythropoiesis, aberrant splicing, and sensitivity to therapeutic spliceosome modulation. *Cancer Cell*. 2016; 30(3):404-417.

44. Kulasekararaj AG, Smith AE, Mian SA, et al. TP53 mutations in myelodysplastic syndrome are strongly correlated with aberrations of chromosome 5, and correlate with adverse prognosis. *Br J Haematol*. 2013;160(5):660-672.